Supplementary Information (SI) for Nanoscale.
This journal is © The Royal Society of Chemistry 2026

Coaxial Spinning $Ti_3C_2T_X$ MXene Fibers with Spontaneous Radial Densification Achieves Simultaneous Improvements in Both Mechanical Strength and Charge Storage Ability

Fanjie Shi,† Henghan Dai,† Ning He, Yang Guo, Yufan Shen, Huifang Wang, Hai Xu,* Yuzhen Wang,* Gengzhi Sun*

Institute of Advanced Materials (IAM), Nanjing Tech University (NanjingTech), 30 South Puzhu Road, Nanjing 211816, China

E-mail: iamxuhai@njtech.edu.cn (H. Xu); iamyzwang@njtech.edu.cn (Y. Z. Wang); iamgzsun@njtech.edu.cn (G. Z. Sun)

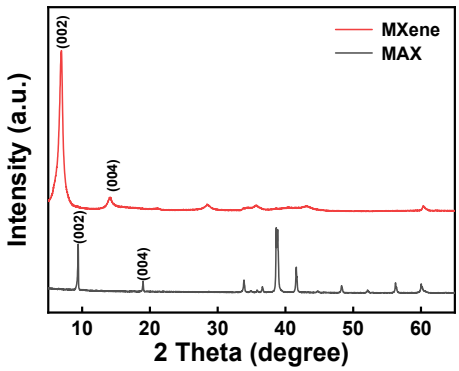

Fig. S1 XRD patterns of precursor Ti_3AlC_2 MAX and $Ti_3C_2T_X$ MXene nanosheets.

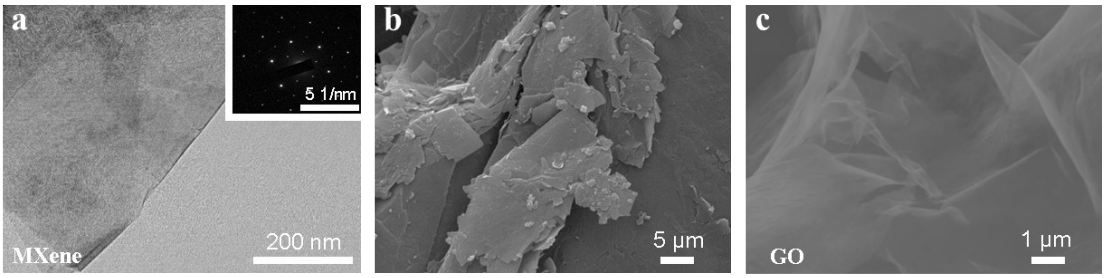

Fig. S2 (a) TEM image of MXene nanosheets (The inset illustration shows the selected area electron diffraction (SAED) pattern. (b) SEM image of Graphite before exfoliation. (c) SEM image of GO nanosheets.

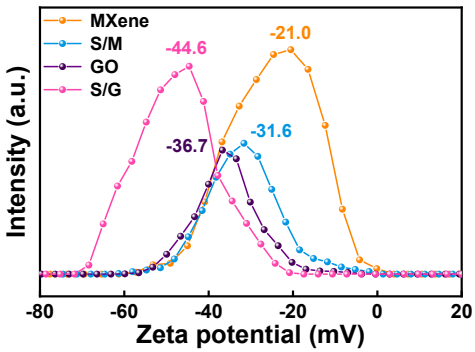

Fig. S3 Zeta potentials of MXene, SA/MXene (S/M), GO and SA/GO (S/G).

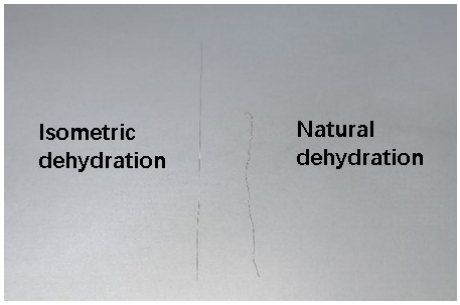

Fig. S4 Photographs of S/M@S/G fibers that are forced to maintain its original length and dried without any restriction during desiccation.

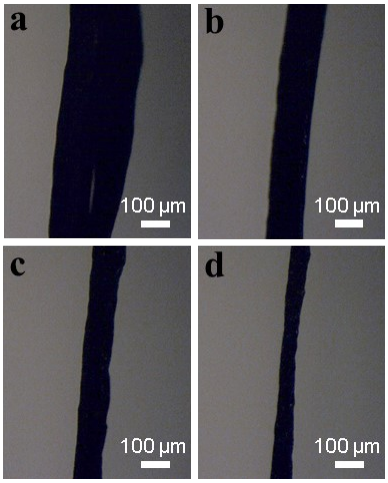

Fig. S5 Photographs of S/M@S/G fiber at different drying time: (a) 2 min (198 μm in diameter), (b) 4 min, (c) 6 min and (d) 8 min (56 μm in diameter).

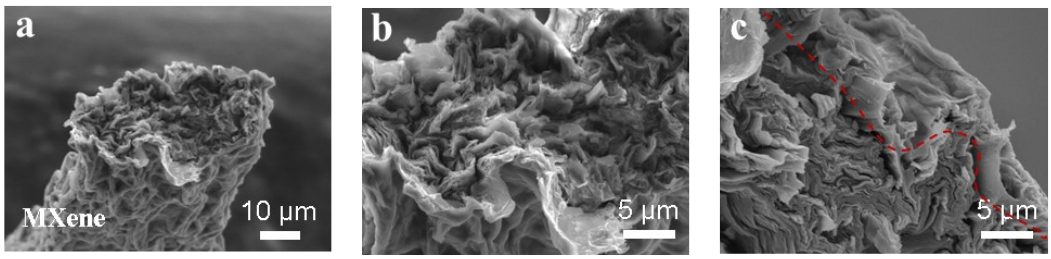

Fig. S6 Cross sectional SEM image of (a) MXene fiber. High-magnification SEM image of (b) MXene fiber and (c) S/M@S/G fiber (The red dotted line is the core and shell boundary line).

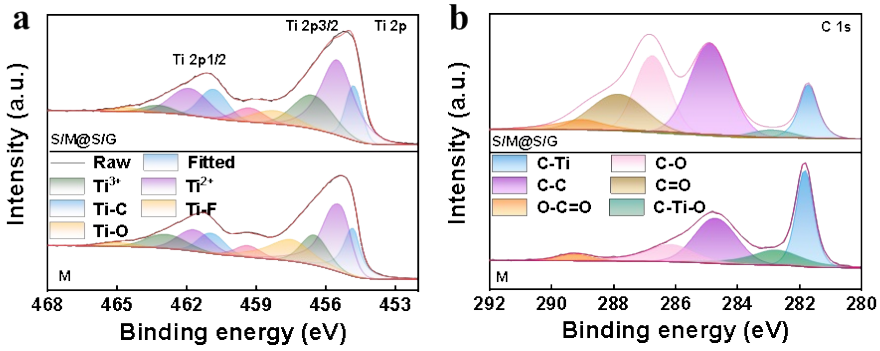

Fig. S7 (a) Ti 2p XPS spectra and (b) C 1s XPS spectra of MXene and S/M@S/G fibers.

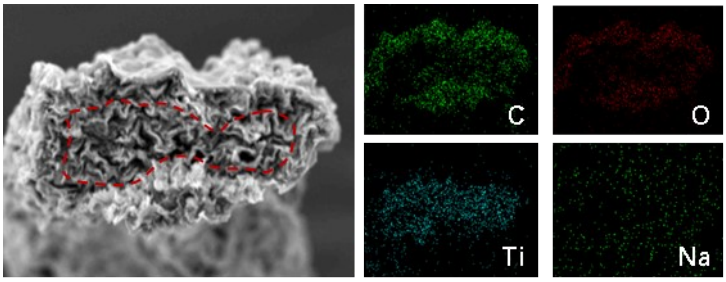

Fig. S8 EDS mapping of S/M@S/G hybrid core-sheath fiber (The red dotted line is the core and shell boundary line).

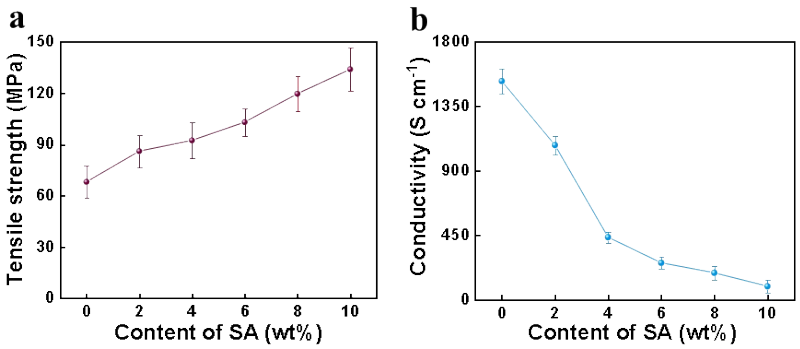

Fig. S9 (a) Tensile strength and (b) Conductivity of S/M fiber with different SA contents.

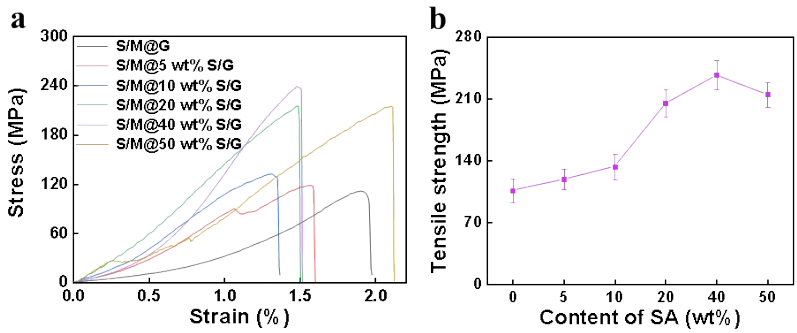

Fig. S10 (a) Stress-strain curves and (b) tensile strength of S/M@S/G fiber with different SA contents in shell.

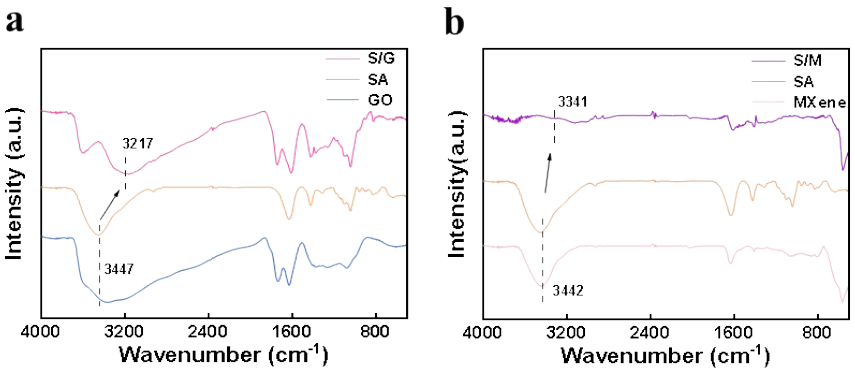

Fig. S11 (a) FT-IR spectra of GO, SA and S/G. (b) FTIR spectra of MXene, SA and S/M.

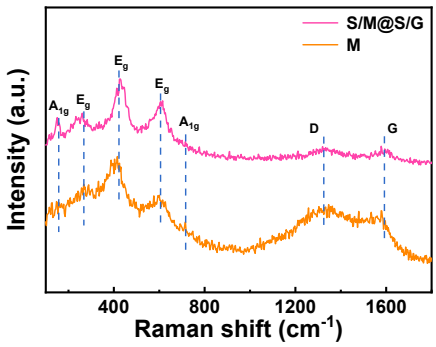

Fig. S12 Raman spectra of pure MXene fiber and S/M@S/G core-sheath fiber.

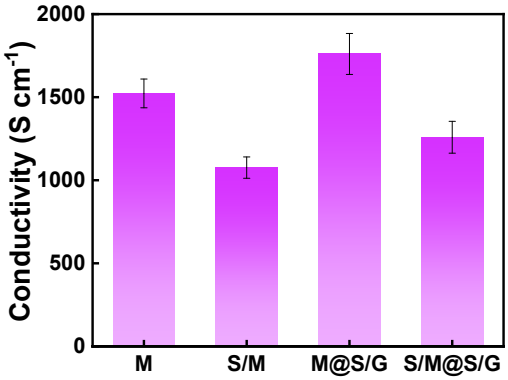

Fig. S13 The conductivity of pure MXene, S/M, M@S/G and S/M@S/G fibers.

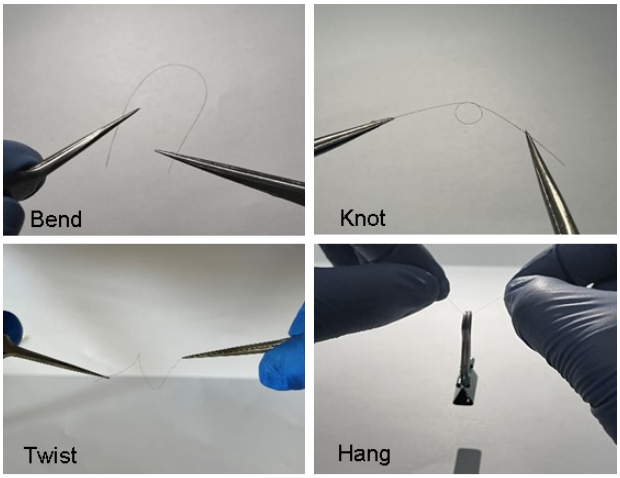

Fig. S14 The mechanical properties of S/M@S/G core-sheath fiber under different conditions.

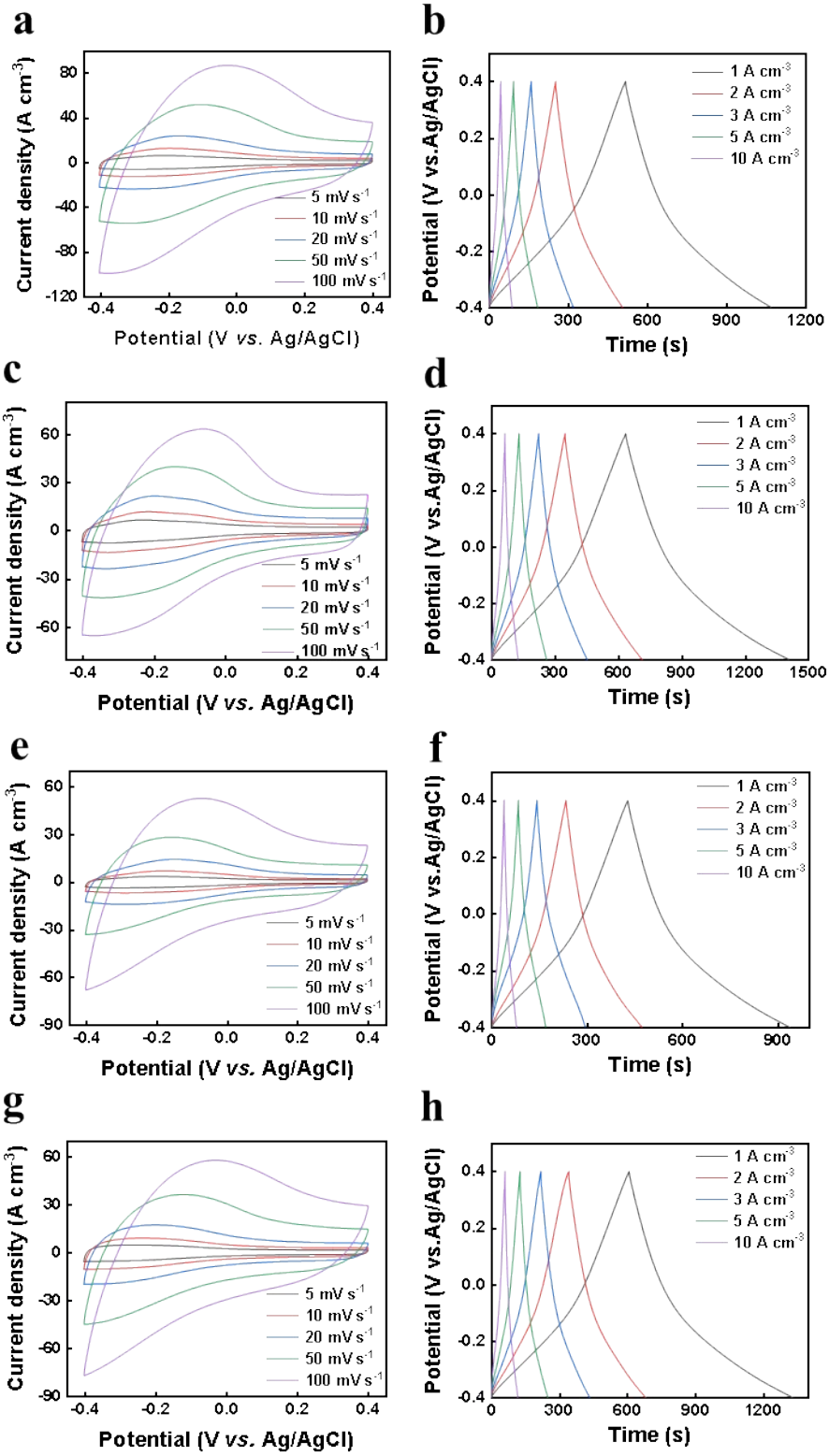

Fig. S15 The CV curves at different scan rates and GCD profiles at different current densities of (a, b) MXene fiber, (c, d) S/M fiber, (e, f) M@S/G fiber and (g, h) S/M@S/G fiber.

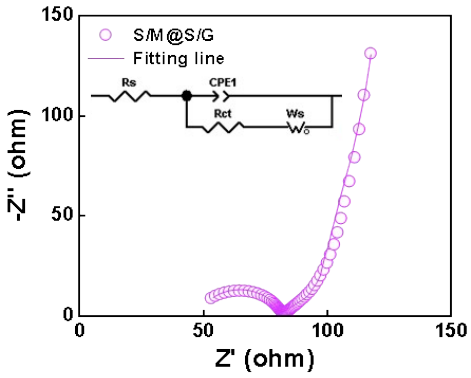

Fig. S16 Nyquist plots of S/M@S/G fiber in two-electrode system.

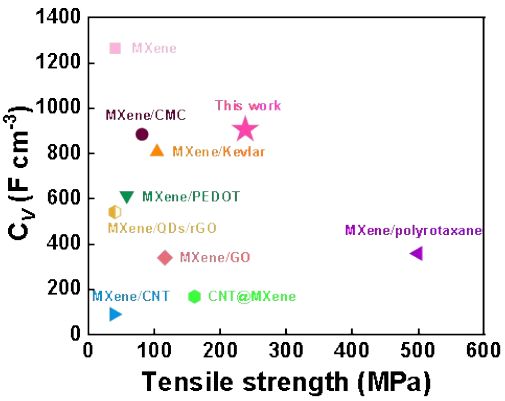

Fig. S17 Comparison of S/M@S/G core-sheath fiber with several previously reported MXene-based fibers regarding tensile strength and volumetric capacitance.

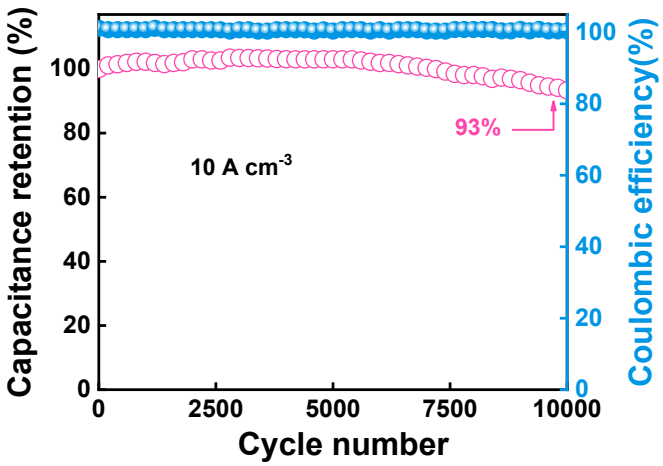

Fig. S18 Stability of S/M@S/G fiber over 10000 cycles at 10 A cm^{-3}.

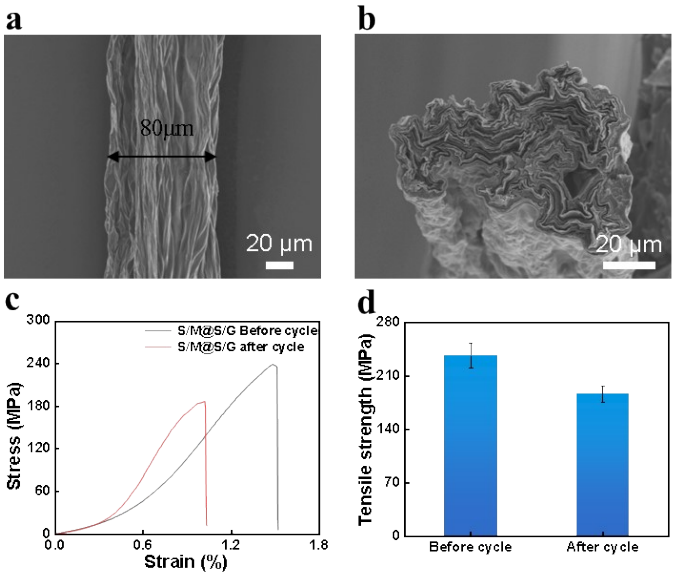

Fig. S19 (a) SEM image and (b) cross section SEM image of S/M@S/G core-sheath fiber (after 10000 charge–discharge cycles). (c) Strain-Stress curves and (d) The Tensile strength of S/M@S/G fiber before and after 10000 cycles.

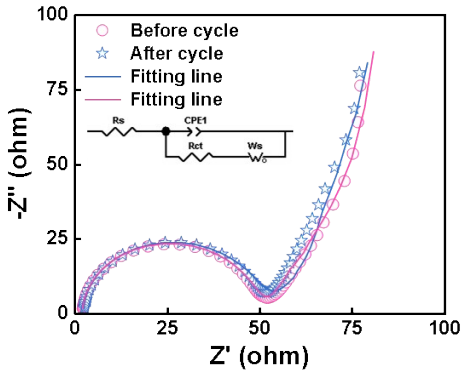

Fig. S20 Nyquist plots of S/M@S/G fiber after 10000 cycles of charge and discharge.

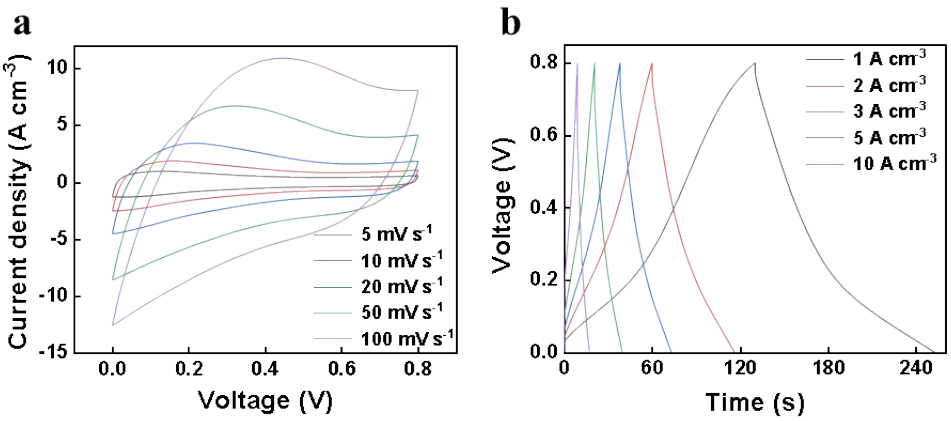

Fig. S21 (a) CV and (b) GCD profiles of FSC based on S/M@S/G fibers.

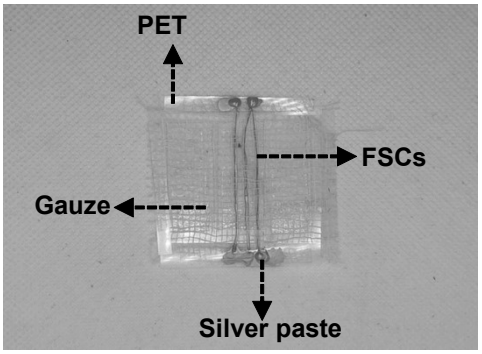

Fig. S22 Photograph of device with several FSCs connected in series (two similar fibers were loaded into the heat shrink tube and gel electrolyte was dropped into the device. The three devices were woven in a piece of gauze. The FSC device was capsulated on a PET substrate).

Table S1: Detailed information and performance comparison of the MXene-based fiber cited in Fig. 3(d and e).

Material	Preparation technique	Tensile strength (MPa)	Toughness (MJ m^{-3})	Conductivity (S cm^{-1})	Ref.
$Ti_3C_2T_x$/CNT	Biscrolling	26.6	2.01	26	36
$Ti_3C_2T_x$/rGO	Wet spinning	110.7	3.8	743.1	32
MXene/GO	Wet spinning	116.1	0.94	72.3	34
$Ti_3C_2T_x$-1	Wet spinning	63.9	0.09	7713	10
$Ti_3C_2T_x$-2	Wet spinning	118	1.09	7200	33
MKB	Wet spinning	242.6	1.0	1412	31
$Ti_3C_2T_x$-nanoyarns	Electrospinning	40	0.27	1195	40
$Ti_3C_2T_x$-PEDOT:PSS	Wet spinning	58.1	0.32	1489	37
$Ti_3C_2T_x$/Cellulose Yarns	Coating	468.4		440	39
S/M@S/G	Wet spinning	238	1.44	1232	This work

Table S2. Detailed information and performance comparison of the MXene-based fiber electrodes cited in Fig. 4(i).

Materials	Testing configuration	C_v (F cm^{-3})	Potential range (V)	Scan rate or current density	Ref.
MXene	three-electrode system platinum mesh Ag/AgCl	759.0	−0.4~0.2	0.5A g^{-1}	55
MXene	three-electrode system carbon rod Ag/AgCl	1265	−0.8~0.2	10 mV s^{-1}	50
MXene/CMC	three-electrode system carbon rod Ag/AgCl	885	−0.6~0.2	1 A cm^{-3}	15
MXene/Kevlar	three-electrode system	807	−0.6~0.2	3 A cm^{-3}	52
MXene/PEDOT	three-electrode system platinum mesh Ag/AgCl	614.5	−0.8~0.2	5 mV s^{-1}	38
MXene/QDs/rGO	three-electrode system	542	−0.2~0.8	0.25 A cm^{-3}	51
MXene/rGO	three-electrode system	415	−0.2~0.4	1 A cm^{-3}	53
MXene/CNT	three-electrode system platinum mesh Ag/AgCl	92	−0.9~0	1 A cm^{-3}	9
MXene/ Polyrotaxane	three-electrode system	360	0~1.0	5 mV s^{-1}	49
S/M@S/G	three-electrode system carbon rod Ag/AgCl	906	−0.4~0.4	1 A cm^{-3}	This work